REPORT DOCUMENTATION PAGE

Form Approved OMB No. 0704-0188

1. REPORT DATE *(DD-MM-YYYY)*	2. REPORT TYPE	3. DATES COVERED *(From - To)*
29/09/2006	Final Report	01/07/2003-31/08/2006

4. TITLE AND SUBTITLE

Subnanosecond Breakdown of Insulating Media

5a. CONTRACT NUMBER

5b. GRANT NUMBER
AFOSR F49620-03-1-0349

5c. PROGRAM ELEMENT NUMBER

6. AUTHOR(S)

Hermann G. Krompholz and Lynn L. Hatfield

5d. PROJECT NUMBER

5e. TASK NUMBER

5f. WORK UNIT NUMBER

7. PERFORMING ORGANIZATION NAME(S) AND ADDRESS(ES)

Center for Pulsed Power and Power Electronics
Texas Tech University

Department of Electrical Engineering
Texas Tech University
Lubbock, Texas 79409-3102

8. PERFORMING ORGANIZATION REPORT NUMBER

AFOSR-2006-1

9. SPONSORING / MONITORING AGENCY NAME(S) AND ADDRESS(ES)

Air Force Office of Scientific Research
801 N. Randolph Street
Room 732
Arlington, Virginia 22203-1977

Dr. Barker

10. SPONSOR/MONITOR'S ACRONYM(S)
AFOSR

11. SPONSOR/MONITOR'S REPORT NUMBER(S)

12. DISTRIBUTION / AVAILABILITY STATEMENT
Unclassified-Unlimited

Distribution Statement A: unlimited

AFRL-SR-AR-TR-06-0391

13. SUPPLEMENTARY NOTES

14. ABSTRACT

Breakdown in argon and air at pressures below one atmosphere, for quasi homogeneous electric fields with amplitudes of up to 3 MV/cm, risetimes < 250 ps, and gap distances on the order of millimeters, is investigated. The setup consists of a RADAN 303 A pulser and pulse slicer SN 4, an impedance-matched oil-filled coaxial line with a lens-transition to a biconical line in vacuum or gas, and an axial or radial gap, with a symmetrical coax arrangement on the other side of the gap. Capacitive voltage dividers allow to determine voltage across as well as conduction current through the gap, with a sampling rate of 50 ps and an analog bandwidth of 6 GHz. Auxiliary diagnostics include x-ray absorber foil spectroscopy, and streak camera imaging. Breakdown is governed by runaway electrons, with multi-channel formation and high ionization and light emission in a thin cathode layer only. In argon and air, time constants for the discharge development have a minimum of around 100 ps at several 10 torr. A qualitative understanding of the observed phenomena and their dependence on gas pressure is based on explosive field emission and gaseous ionization for electron runaway conditions.

15. SUBJECT TERMS
Electrical breakdown, Subnanosecond breakdown, Fast rising pulses.

16. SECURITY CLASSIFICATION OF: NONE			17. LIMITATION OF ABSTRACT	18. NUMBER OF PAGES	19a. NAME OF RESPONSIBLE PERSON
a. REPORT	b. ABSTRACT	c. THIS PAGE	unlimited	17	Hermann G. Krompholz
					19b. TELEPHONE NUMBER *(include area code)* 806-742-3468

1. Introduction

Newer developments in the field of high speed/high power electromagnetics applications, such as Ultrawideband (UWB) radar, plasma limiters, and fast general purpose pulsed power applications, require high power switching times far below one nanosecond. Information about switch closure times and standoff voltages for short pulses is of relevance for many switching and insulation tasks, for both volume breakdown in different media as well as for surface discharges along interfaces.

The technology for achieving these switching times is mainly based on empirical studies, and the understanding of the basic physical processes is limited. High pressure gas switches, with N_2 or H_2, for example, have been shown to produce risetimes on the order of 50 to 200 ps [1, 2, 3], and their principle of operation is described in terms of standard gas breakdown, i.e. the Townsend and streamer mechanism.

The physics background for breakdown caused by short pulses with high overvoltages is far from being clear. Some publications from the 1960's on delay times include the work of Felsenthal and Proud [4]. Physical models discussing streamer development under electron runaway conditions have been introduced by Kunhardt and Byszewski [5, 6, 7], and experimental data on the development of breakdown current and x-ray emission due to fast electrons in nanosecond pulses of several 10 kV amplitude have been given by Byszewski [8 ,9]. More recent work originated prevalently from Russia, and emphasizes the role of runaway electrons for discharges in relatively low pressure gases [10, 11, 12].

For rep-rated operation, special subnanosecond breakdown phenomena, such as corona discharges, act as limiting mechanisms. These discharges, their ignition and re-ignition are also not understood. It is not clear how much energy is dissipated by these discharges, and how they can be avoided. The investigation of sub-nanosecond breakdown opens a way to investigate corona discharges as well, provided that rep-rated sub-nanosecond pulsers are available. Some information on the recovery behavior of fast gas switches can be found from indirect measurements of the electron density vs. time, mainly by measuring the luminosity of the recombining plasma for a long time scale.

The recent availability of high-voltage pulsers reaching into the several 100 kV regime with risetimes of less than 300 ps [13, 14], and of transient digitizers with risetimes down to 100 ps enables exploration of breakdown at higher voltages and shorter pulse risetimes than several years ago. A crucial element is the application of a high voltage pulse to a test gap, with the goal to minimize risetime limitations due to capacitance and changes in geometry. Some attempts have been made to design and investigate fast switching devices using transmission lines and special matching techniques for coaxial line to gap, such as the use of biconical transmission line sections and lenses to minimize pulse distortion [15, 16].

This project concentrated on UWB aspects of fast discharges, where both switching and avoiding corona-like discharges in atmospheric and sub-atmospheric pressure are of interest. The parameter space covered gap widths on the order of one millimeter in a pressure of several torr up to one atmosphere in argon as a model gas, and in air. Amplitudes of voltages applied to the gap were between 80 and 300 kV for quasi homogeneous fields, and 5 kV for tip plane geometry. Both volume discharges and discharges along Lexan surfaces were investigated. Diagnostics include the measurement of voltage across

the gap and conduction current through the gap, x-ray diagnostics using metal foil absorption techniques for quantum energies covering the range up to 150 keV, optical diagnostics using a streak camera with several 10 ps resolution to characterize the discharge channel dynamics, and supplementary measurements of the afterglow emission of visible light yielding information about the initial electron density and recovery behavior. Simple modeling has been performed describing the transition from vacuum discharge to gaseous collisions and charge amplification processes supporting the major experimental findings.

Results of this project reveal the basic mechanisms leading to gas breakdown in the sub-nanosecond time regime. Over the whole parameter space the breakdown is governed by runaway electrons. Statistical time delays are not observed, from which we infer a discharge starting process due to electron field emission. With increasing pressure, space charge effects due to gaseous ionization are expected, providing a transition from a Townsend-like discharge to streamer. The discharge structure and the amplification mechanisms are different from standard discharges, however. Fast acceleration of electrons to energies at which the cross-sections are strongly decreasing leads to energy dissipation in a thin cathode layer only, and the short development times of the channels provide a decoupling of individual channels and multi-channel breakdown. The experimental results have been complemented by simple modeling using the "average force equation" in the strong runaway regime. Together, they provide a way to model breakdown, and deliver a data base which will be highly valued by several research groups working in the field of applications of fast switching.

2. Methodology

2.1 Setups

During the course of this project, three different setups have been used. Common to all setups is the use of a high voltage pulser, connected via a transmission line to a test gap in controllable atmosphere, and a second transmission line on the other side of the gap simulating a matched load.

Setup #1. In the initial phase, a Bournlea pulser with about 5 kV amplitude served as a source for tests with a tip-plane geometry, with extremely inhomogeneous electric fields in the gap. This work represented the continuation of AFOSR-funded previous projects from about 2000 to 2004 [17 - 21].

Setup #2. The availability of a RADAN 303 A pulser with pulse slicer SN 4 enabled the investigation of breakdown for quasi-homogeneous fields for both volume and surface breakdown with pulser voltages up to 150 kV. [22, 23].

Setup # 3. This setup was improved in the third phase to a custom-build oil-filled transmission line coupled via a dielectric lens to a biconical line connected to the gap. This setup represents the achievable optimum with respect to minimizing pulse distortion and still providing accessibility for a variety of diagnostics methods. [24]

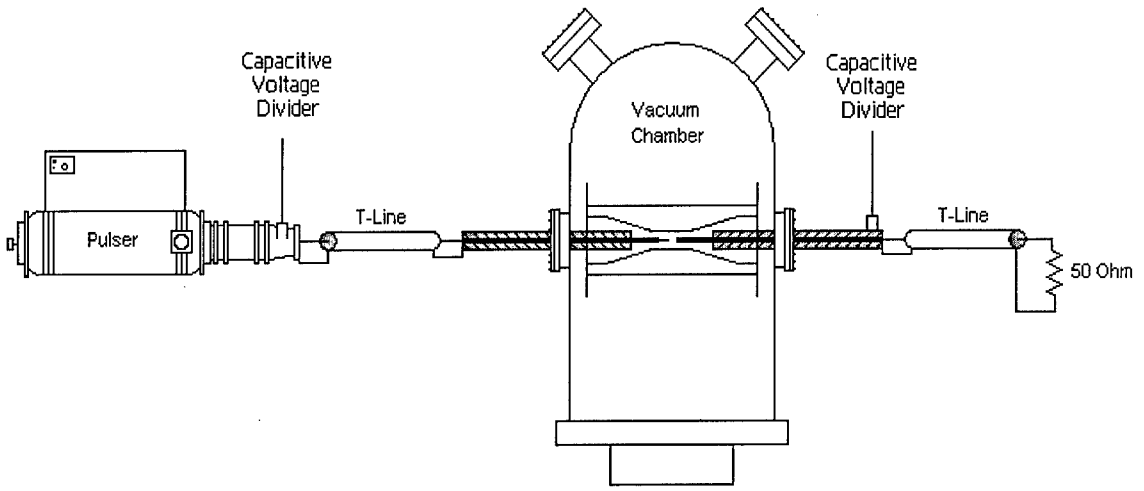

Fig. 1. Basic setup for tip-plane geometry (Setup # 1, with Bournlea pulser) with RG-19 coax lines. The same basic arrangement was used with flat electrodes and RADAN pulser (Setup #2)

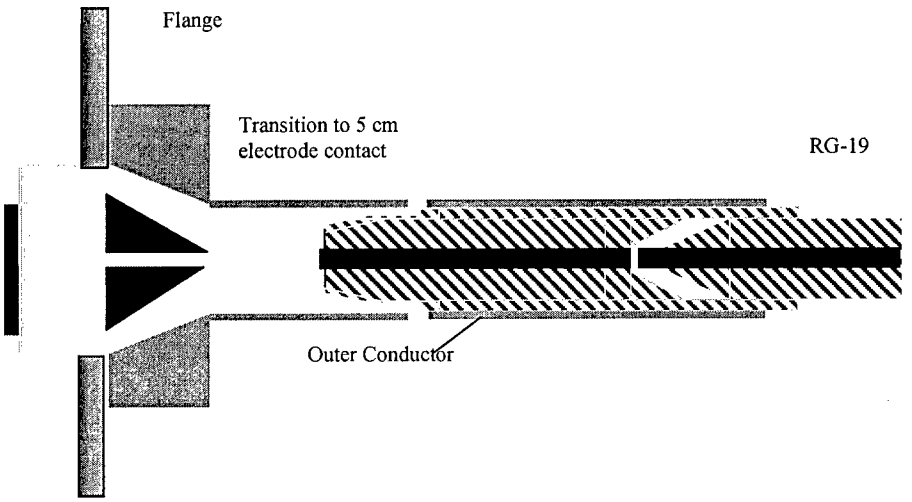

Fig. 2. Feedthrough arrangement used for setup in Fig. 1

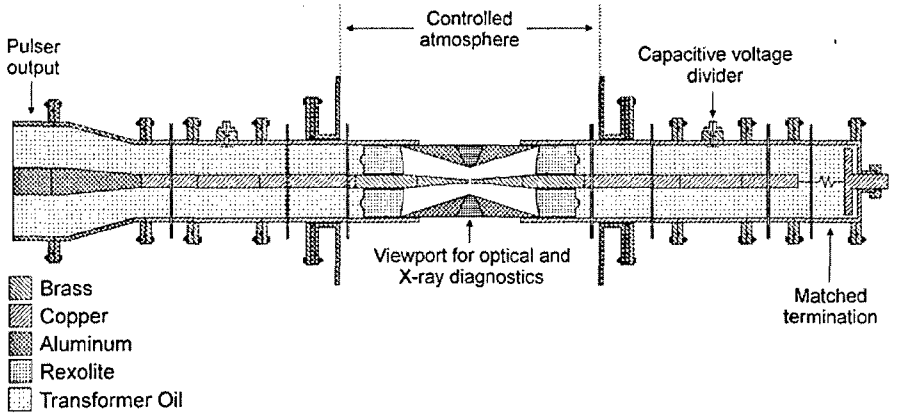

Fig. 3. Setup #3 with oil-filled transmission lines, and lens transition from coaxial to bi-conical line. Not to scale, overall length 5 m, outer diameter of coax 4 cm.

2.2 Diagnostics

Common in all setups for electrical diagnostics was the use of capacitive voltage dividers integrated into the transmission lines at positions which allowed separation of incident and reflected pulses on the input line. These dividers provide a risetime of several 10 ps, a droop on the order of several 10 ns, and they limit the risetime of the transmitted signal (i.e. signal propagating along the transmission line after crossing the divider) again to several 10 ps. In conjunction with the digitizer used, Tektronix TDS 6604 with 50 ps sampling time and 6 GHz analog bandwidth, these dividers seem to be the ideal line voltage monitor, much more suitable than e.g. shunts or magnetic current sensors which would cause much larger signal distortion on the main line.

The voltages traveling on the transmission lines, i.e. incident and reflected voltage on the input side, and transmitted voltage at the output side, allow the determination of gap voltage and gap conduction current, and especially their temporal correlation [23, 24]. The accuracy of this determination is limited by noise following the main pulse from the RADAN, and by reflections on the transmission lines, especially at feedthroughs, used in the second-phase setup with standard transmission lines. The signal disturbances due to non-ideal transmission lines have been virtually eliminated for the last setup, at least as far as the pulse application to the gap and the measurement of the transmitted pulse is concerned.

To quantify the role of fast electrons in the discharge, a standard x-ray diagnostics method is used to measure the spatially integrated intensity and to estimate the spectral distribution with absorber foil, plastic scintillator (Bicron BC 404), and photomultiplier tube (Hamamatsu R 1828-01, nominal amplification 3×10^7). Neutral density filters have been used to limit the photomultiplier to its linear range. The decay time constant of this system is about 2 ns, and the x-ray measurements have to be considered time integrated. Details are described in the pertinent publications [23, 24].

Information about the discharge channel structure and dynamics was obtained using a Hadland Imacon 500-100 streak camera, with image tube PV001/S20uv. A line perpendicular to the discharge axis was imaged onto the entrance slit of the camera with 4-fold magnification, and streak speeds down to 50 ps/mm were used. Portions around the cath-

ode, the center of the gap, and anode were imaged separately. In a second set of images, the entrance slit was placed along the discharge axis in the center.

3. Results

3.1 Breakdown voltage and breakdown time constants

For the majority of the measurements electrical diagnostics only were used. Detailed results are described in the references 20-24. The following discussion concentrates on items which have not been published in detail yet. In virtually all cases, breakdown occurred during the rising portion of the applied voltage, which makes the definition of breakdown voltage and breakdown delay time somewhat ambiguous. We define the following time constants, cf. Fig. 4:

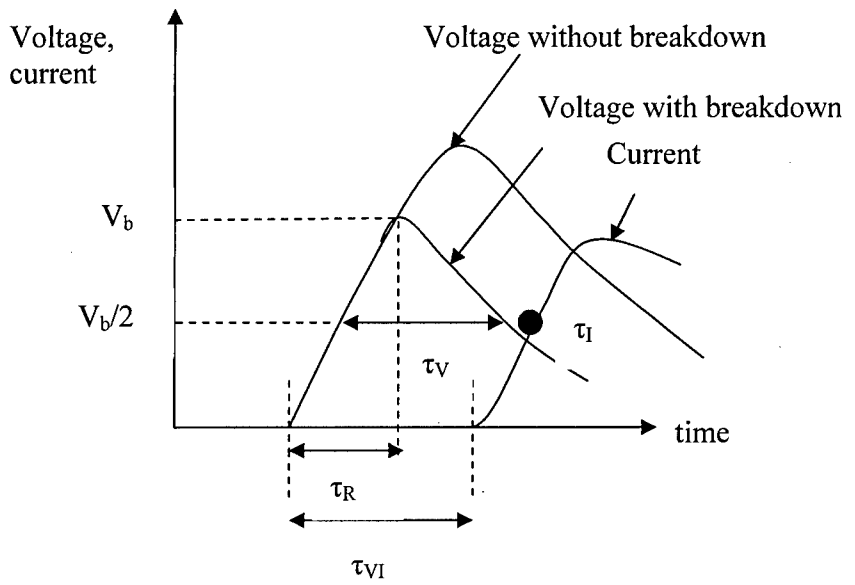

Fig. 4. Generic signals of voltage across the gap and current through the gap. V_b breakdown voltage, τ_R voltage risetime, τ_V FWHM of voltage, or switching time, τ_{VI} voltage-current delay time, τ_I=I/(dI/dt) current amplification time

The following two figures, Fig. 5 and 6, show the breakdown voltages for 40 kV and 100 kV pulser voltage, measured with setup #3 for an axial gap with voltage doubling. These pseudo-"Paschen"-curves confirm the general tendency for the shift of the pressure at which the voltage attains a minimum to larger values for increasing amplitudes of the applied field (or increasing dV/dt) [25, 26]. Compare also Fig. 4 in ref [23].

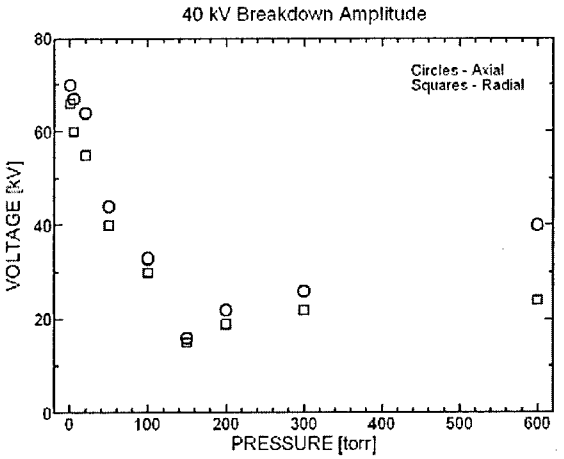

Fig. 5. Breakdown voltage for argon, with 40 kV pulser amplitude

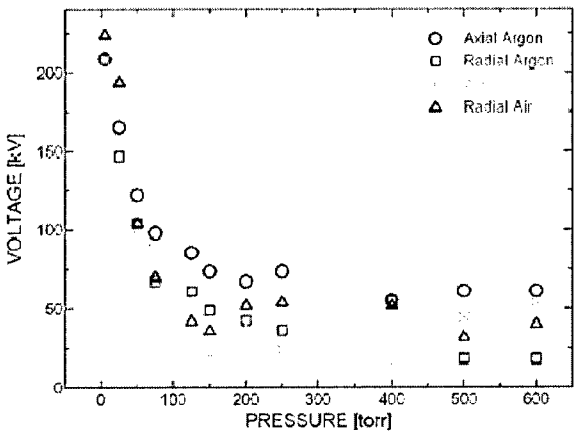

Fig. 6. Breakdown voltage for argon and air with 100 kV pulser amplitude

Breakdown voltages for surface flashover differ from the ones for volume breakdown (cf. Fig. 4 in ref [23]) and show a pronounced minimum at several torr, which might be associated with a difference in the charge carrier amplification mechanism, where secondary electrons and outgassing are expected to play a major role.

Minimum breakdown voltages are associated with minimum discharge development times, see Fig. 7 as an example. These data were obtained with setup #3 and an axial gap, where a parasitic discharge developed radially after a pressure-dependent time delay. The axial discharge is considered to be the primary discharge with "standard" breakdown, whereas the radial discharge seems to be triggered by the axial one.

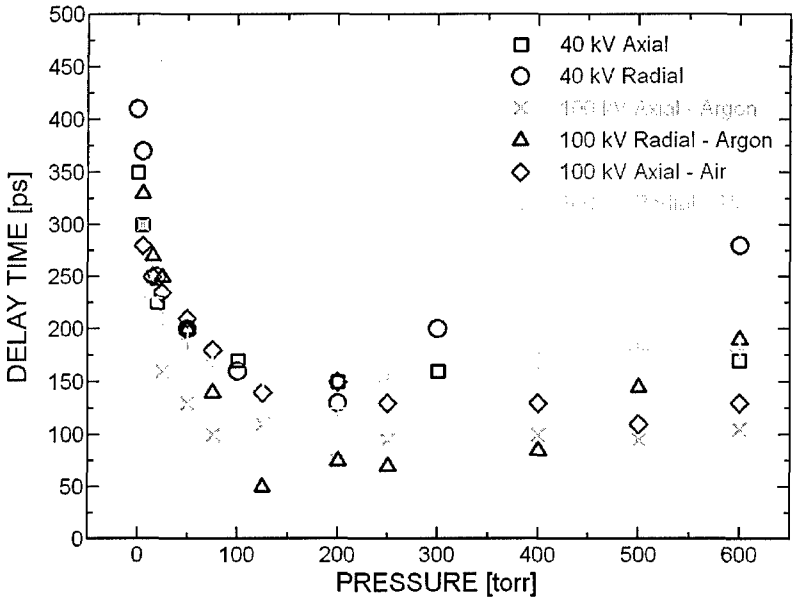

Fig. 7. Delay times between voltage and current for 40 and 100 kV pulser amplitude

The time constant τ_I=I/(dI/dt) is obviously the most relevant for the description of the discharge "physics". Unfortunately, it has to be found from difference and differential operations on the originally measured signals, and the accuracy of its determination is limited by noise as well as by the somewhat insufficient sampling rate. Examples for radial breakdown (cf. [23]) show τ_I-values varying between 300 and 50 ps at pressures below 20 torr, and are in the range of 180±30 ps for higher pressures. With axial breakdown (which means a factor of four faster gap capacitance charging than for radial breakdown), this time constant is by about a factor of 3 smaller, cf. Fig. 8.

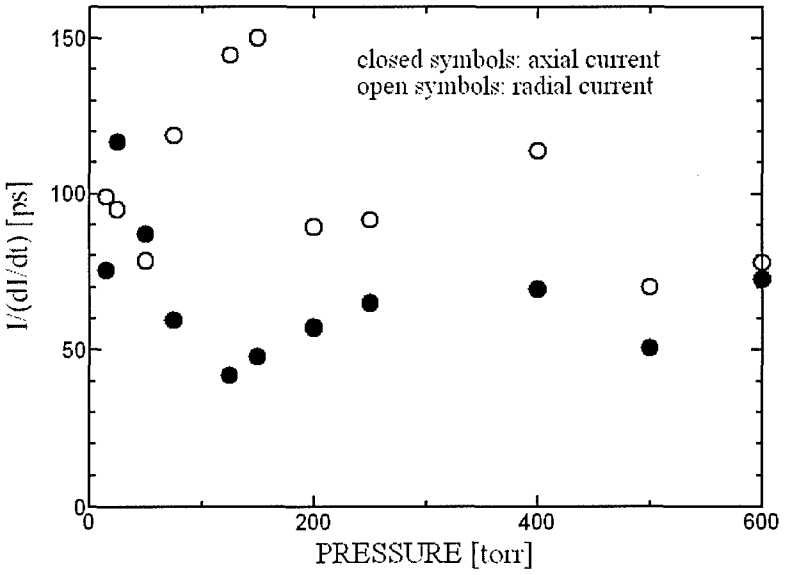

Fig. 8. Time constant τ_I for argon and 100 kV pulser voltage, measured with setup #3.

3.2. X-ray emission

Preliminary x-ray measurements with low resolution and relatively high PMT noise level have been done with setup #2 and are described in [23]. They show that relatively hard x-rays (E> 30 keV) are emitted for pressures up to 150 torr. An improved setup with largely reduced noise level was used to measure the x-ray emission for setup # 3, for axial discharges, with results shown in [24]. These measurements show the extension of hard x-ray emission (> 50 keV) to almost atmospheric pressure. A problem with these measurements was parasitic radial discharges with probably varying position of the x-ray source, which makes the quantitative evaluation of the measured spectra somewhat uncertain. In a third set of experiments, a radial discharge was used, for which the position uncertainty is eliminated. Since these results have not been published yet, they are described in some detail in the following.

Fig. 9 shows the sensitivity curves (i.e. foil transmission times scintillator absorption) of the arrangement used, and the measured PMT signals with a pulser voltage of 150 kV. The large variation of the signal amplitudes has been compensated with neutral density filters to assure PMT operation in the linear regime. Data points represent averages and standard deviations of 5 discharges. The sensitivity curve for lead is about a factor of 10 below the one for silver, and covers about the same spectral range, due to the rather large transmission above the L-edge. The noise level due to noise produced by the pulser and coupled to the PMT signal at the time of x-ray emission has a signal amplitude of about 0.1 V, which defines the threshold for the x-ray measurements. A discrimination of energies substantially larger than 60 keV is difficult, since all metallic elements with atomic numbers larger than the one of silver have their L-edges in the region of 60 to 80 keV. Note that the good reproducibility of the discharges allows to characterize the x-ray spectrum from multiple shots.

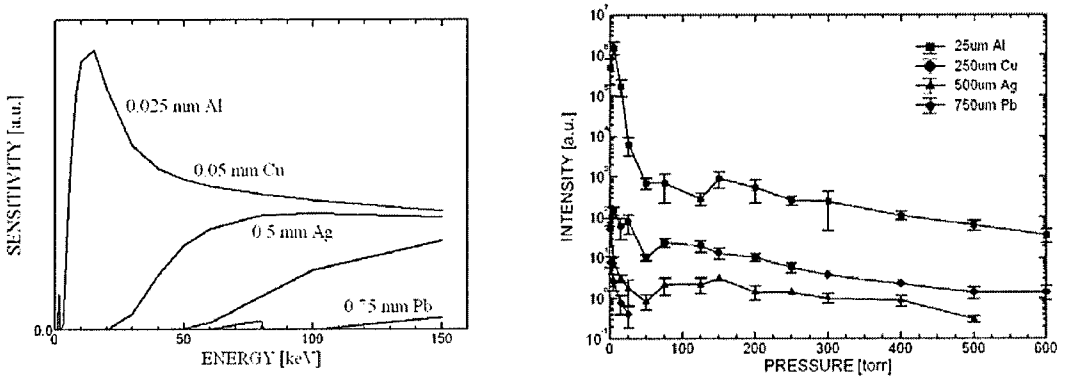

Fig. 9. Left: Spectral sensitivity for the x-ray measurements with 0.02 mm Al, 0.25 mm Cu, 0.5 mm Ag. Right: Measured x-ray signal amplitudes with different absorber foils, as a function of pressure

The absorber foil materials and thicknesses have been chosen so that they define different energy bands, 5 to 20 keV, 20 to 50 keV, and 50 keV to the maximum possible energy of 150 keV, the pulser voltage. This upper value might be reduced to the actual breakdown voltage. There are some hints in the literature [11], however, that polarizing

self acceleration might lead to electron energies exceeding the equivalent of the applied voltage. Assuming pure Bremsstrahlung emission allows to estimate the electron energy distribution. Radiation in the upper energy band is obviously caused by electrons with at least 50 keV energy. The number of these electrons or the corresponding x-ray signals for Ag-absorber is small compared to the x-ray intensity or electron number in the center band, so that the 0.25 mm Cu curve represents the number of electrons in the center band. The same argument applies for the transition from the center band to the lowest energy band. As a consequence, the x-ray intensity curves represent the approximate relative number of electrons in the corresponding energy bands. A more detailed quantitative analysis, based on the linearly decreasing bremsstrahlung spectrum of monoenergetic electrons, and the superposition of three groups of electrons, confirms this statement.

3.3. Spatial discharge structure [23]

Streak camera pictures were recorded with the slit perpendicular to the discharge axis, with slit widths of 100 μm, and the slit positioned just above the cathode, the center of the gap, and above the anode surface. Typical examples are shown in Figure 10.

At low pressures, around 10 torr, the discharge is rather diffuse and covers the whole cathode area. For higher pressures, individual channels can be seen with diameters on the order of 1 mm. Initial channel expansions last about 200 ps, and the expansion velocity is approximately 2.5×10^8 cm/s. The tendency for simultaneous development of multiple channels increases with pressure. Images with the slit at the center of the gap, or in the vicinity of the anode, show similar structures with slightly larger diameters, but with intensities one to two orders of magnitude lower than the ones in the vicinity of the cathode. Also, a channel expansion was not observed at these positions, the channel diameter starts out with finite size and is constant in time.

Figure 11 shows streak images with the slit parallel to the discharge axis. A rather large slit width of 2 mm has been chosen to capture the channels which vary in position for almost every discharge. A sharply bounded region with high luminosity can be seen in the cathode vicinity (more pronounced at higher pressure), and a region with constant low level luminosity in the rest of the gap. Propagation velocities vary between 5×10^8 cm/s for low (<100 torr) and high (>300 torr) pressure and 10^9cm/s for intermediate pressure (100 to 300 torr).

Further streak pictures have been taken with air, and they do not show any discernable differences to the ones in argon. Pictures with slower streak speed show that the discharge channels – after the build-up phase lasting a fraction of a nanosecond, are virtually stationary for at least several 100 ns after the end of current flow, with decreasing intensity versus time.

3.4 Luminosity and afterglow

The detailed results of luminosity measurements and estimations of the electron density using rate equations can be found in [23]. The essential feature is a slow plasma decay,

where after 1 μs electron densities on the order of several 10^{12} cm^{-3} are still present. This observed slow recombination rate might impose limitations on high repetition-rate operation.

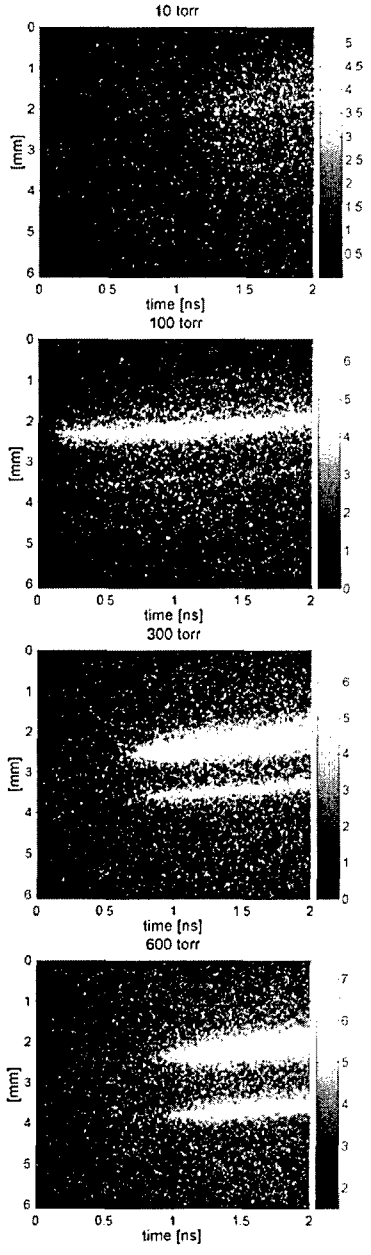

Fig. 9. Streak pictures with slit perpendicular to the discharge axis, close to the cathode, for argon gas pressures (from top to bottom) of 10, 100, 300, and 600 torr. The time range (horizontal) extends over two nanoseconds, the spatial scale (vertical) covers 6 mm. Electrode diameter was 6 mm. Deviations of the traces from the horizontal are due to a slight internal misalignment of the camera. A logarithmic intensity scale has been used to better show the discharge structure.

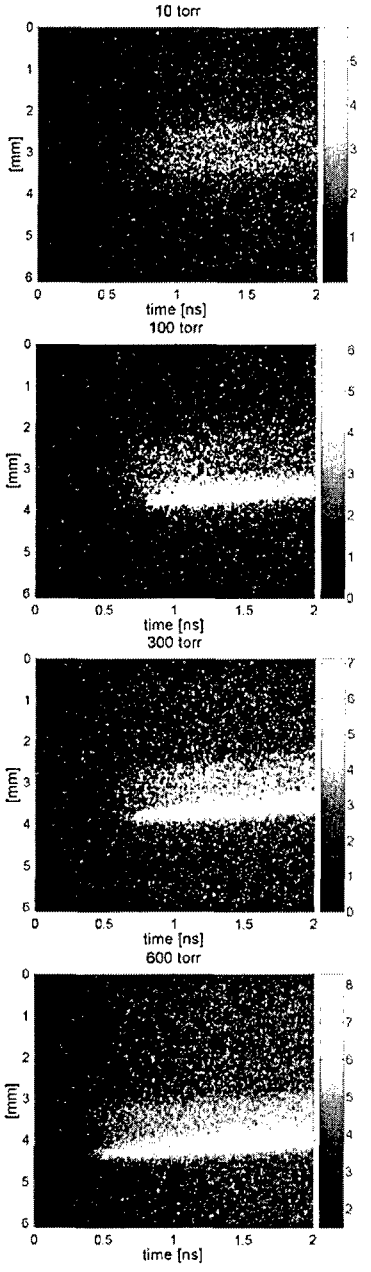

Fig. 10. Streak images with slit parallel to the discharge axis, slit width 2 mm. Cathode at lower limit of luminous region, anode at upper limit, with gap width 1 mm. Time range 2 ns, spatial scale 6 mm. Same pressures and arrangement as in Fig. 9. Discharges in argon. A logarithmic intensity scale has been used to better show the discharge structure.

3.5 Modeling

In order to get in-principle information about the behavior of electrons during discharge initiation, a rough calculation based on the average force-equation was carried out. Details can again be found in [23]. Fig. 12 shows, as an example, the pressure at which electrons emitted from the cathode arrive at the anode with more than 90 % of the available energy (elementary charge x gap voltage). The reduced runaway field would be E/p = 2.3×10^3 V/(cm torr). Literature data [11] indicate values which are about one order of magnitude smaller, but these values are related to the threshold of runaway, i.e. when a small fraction of thermally distributed electrons reach runaway conditions. Fig. 13 shows the number of ionizing collisions per electron emitted from the cathode, and Fig. 14 depicts the average position of ionizing collisions. We conclude that a transition from Townsend to streamer breakdown occurs at a field dependent pressure (e.g. where the number of ionizing collisions equals unity in Fig. 13) which varies from 10 torr at 30 kV applied voltage to 80 torr at 150 kV. The thickness of the primary ionization layer remains independent of pressure and for voltages between 30 and 150 kV, less than 0.2 mm. For a further discussion, especially on the possible transition to streamers under runaway conditions, see [23].

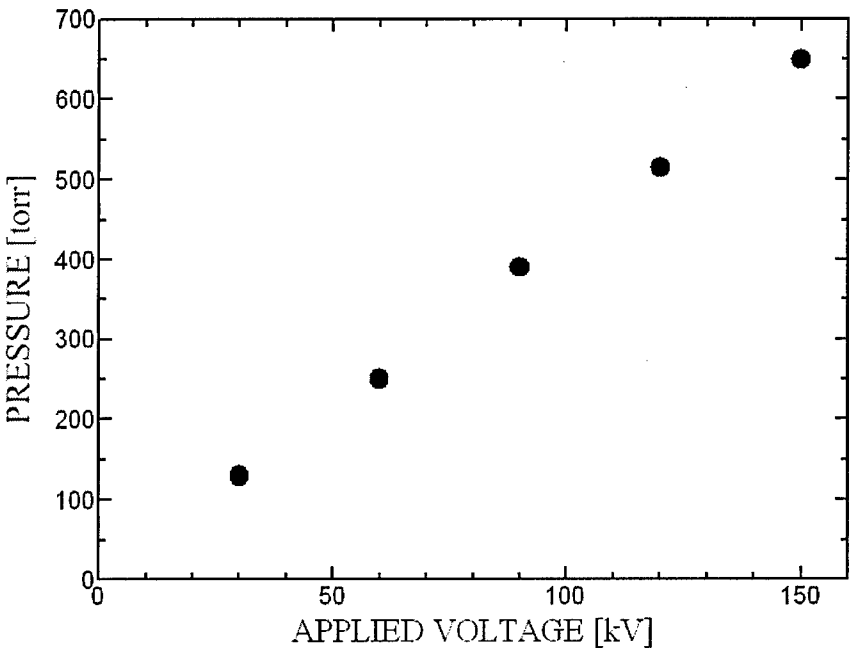

Fig. 12. Pressure at which the electron arrival energy is 90 % of the gap voltage, for a gap distance of 1 mm, argon

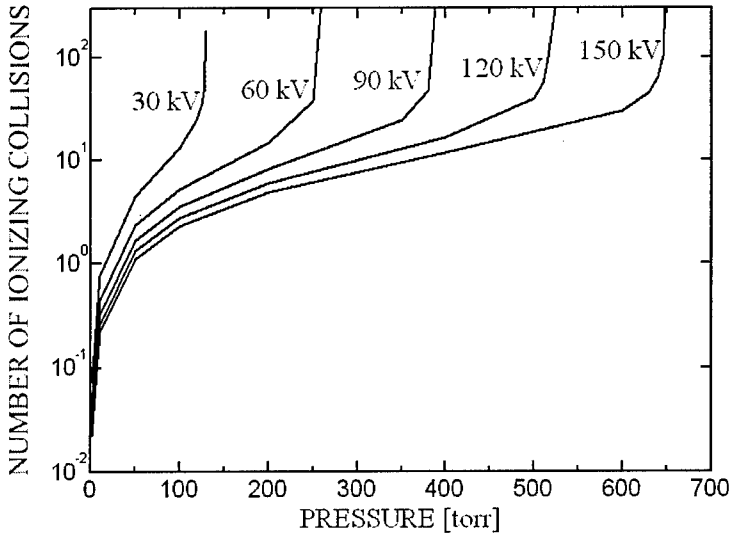

Fig. 13. Number of ionizing collisions per primary electron, as a function of pressure for a gap width of 1 mm. Parameter is the applied voltage.

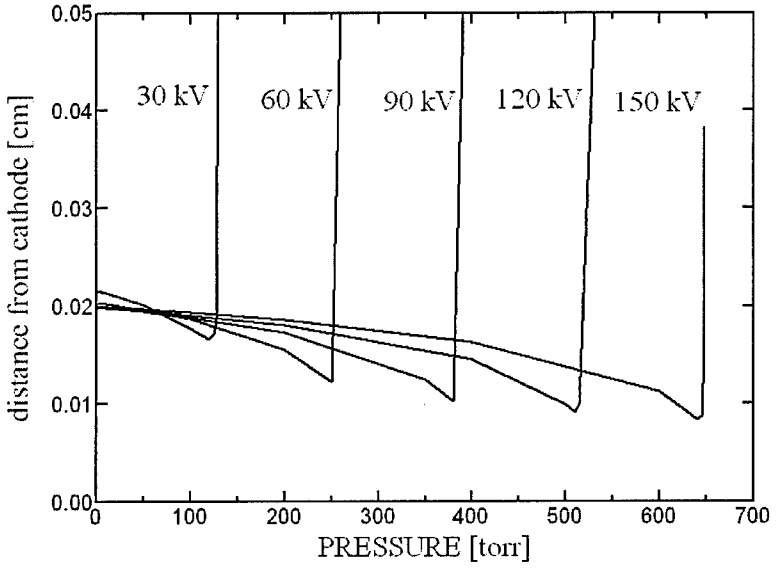

Fig. 14. Average position for ionization, i.e. $\int w_i(x)xdx / \int w_i(x)dx$, where w_i is the number of ionizations per unit length, and the integration extends over the gap width from cathode to anode. Parameter is the applied voltage.

4. Discussion and conclusions

Gaseous breakdown and breakdown along lexan-surfaces in gaseous environment at pressures below one atmosphere were investigated using voltage pulses with 200 ps risetime, 300 ps duration, and amplitudes between 40 and 300 kV. With a specially designed system consisting of coax lines coupled via dielectric lenses to biconical lines, these pulses could be applied distortion-free to test gaps with a gap width on the order of millimeters.

Breakdown occurs in virtually all cases during the rising part of the pulse, with breakdown voltages and delay times having a minimum of about 100 ps at pressures of 10 to 100 torr. Current amplification times I/(dI/dt) can be as short as 50 ps. The general scaling law, i.e. E/p as a function of $p\tau$ [4, 26], where τ is the discharge development time, is still valid for our parameter regime, see Fig. 15. Breakdown curves, i.e. breakdown voltage as a function of pressure for constant dV/dt, show a Paschen-curve like behavior, with a shift of the pd minimum to higher values if dV/dt is increased.

Physical mechanisms for ultrafast breakdown are dominated by runaway electrons, where a substantial number of electrons is accelerated to energies which correspond to the breakdown voltage. Previous investigations and simple modeling have shown, that runaway conditions exist for the whole pressure range of our investigations, and that the main amplification happens in the vicinity of the cathode. We expect associated space charge fields to increase field emission of electrons from the cathode, starting at several 10 torr [23].

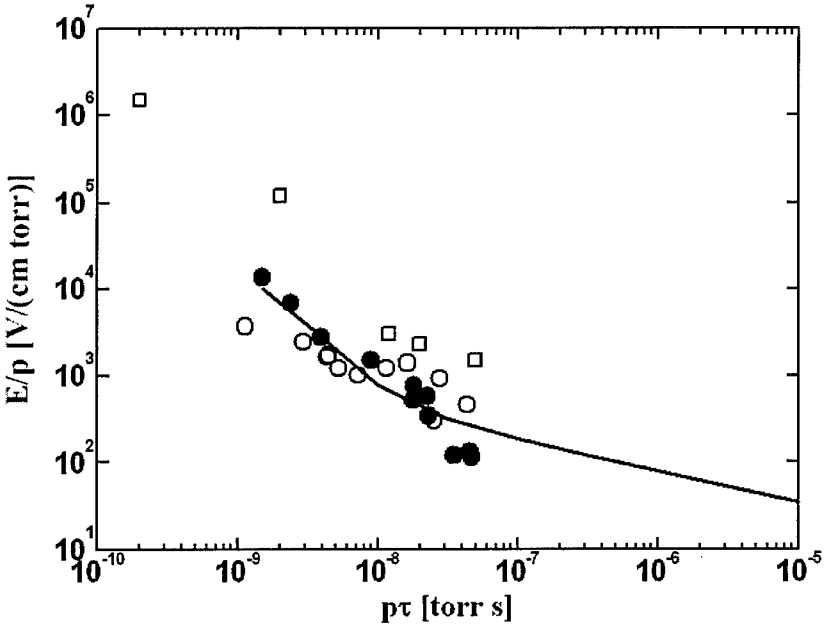

Fig. 15 Scaling law E/p vs. $p\tau$. Circles: data points from Fig. 7, Squares; argon, 150 kV from [23], Line: from [4]

5. References

[1] W.R. Cravey, E.K. Freytag, D.A. Goerz, P. Poulsen, P.A. Pincosy, "Picosecond high pressure gas switch experiment", Proc. 9th International Pulsed Power Conference 1993, pp. 483-486.
[2] L.H. Bowen, E. G. Farr, J.M. Elizondo, J. Lehr "High-voltage, high rep-rate, low jitter, UWB source with ferroelectric trigger", Proc. 12th IEEE Int. Pulsed Power Conference 1999, pp. 1137-1140.
[3] A.R. Dick, S.J MacGregor, M.T. Buttram, R.C Pates, L.F. Rinehart, K.R Prestwich, "Breakdown phenomena in ultra-fast plasma closing switches", Proc. of 12th IEEE Int. Pulsed Power Conference 1999, pp. 1149-1152.
[4] P. Felsenthal and J.M. Proud, "Nanosecond-Pulse Breakdown in Gases", Phys. Rev., vol. **A139,** pp. 1797-1804, 1965.
[5] E.E. Kunhardt, W.W. Byszewski, "Development of overvoltage breakdown in high gas pressure", Phys. Rev., vol. **A21,** pp. 2069-2077, 1980
[6] E.E. Kunhardt, Y. Tzeng, "Development of an electron avalanche and its transition to streamers", Phys. Rev., vol. **A38,** pp. 1410-1421, 1988.
[7] E.E. Kunhardt, Y. Tzeng, J.P. Boeuf, "Stochastic development of an electron avalanche", Phys. Rev., vol. **A34** pp. 440-449, 1986.
[8] W.W. Byszewski, M.J. Enright, J.M. Proud, "Transient development of nanosecond gas discharges", IEEE Transactions on Plasma Science, vol. **PS-10,** pp. 281-285, 1982.
[9] W.W. Byszewski, G. Reinhold, "X-ray diagnostics of runaway electrons in fast gas discharges", Phys. Rev., vol. **A26** pp. 2826-2831,. 1982.
[10] V.F. Tarasenko, S.I. Yakovlenko, "High power subnanosecond beams of runaway electrons generated in dense gases", Physica Scripta, Vol. 72, 41-67, 2005
[11] L.P. Babich, "High-Energy Phenomena in Electric Discharges in Dense Gases", ISTC Science and Technology Series, Vol. 2, Arlington, VA: Futurepast, Inc., 2003
[12] I.D. Kostyrya, V.S. Akakun, V.F. Tarasenko, A.N. Tkachev, S.I. Yakovlenko, "The role of fast electrons in the formation of a pulsed volume discharge at elevated gas pressures", Technical Physics Letters, Vol. **30**, No. 5, 2004, pp. 411-414
[13] G. Mesyats, V. Shpak, M. Yalandin, and S. Shunailov, "Compact High-Current Accelerators Based on the Radan SEF-303 Pulsed Power Source", Proc. of 9th IEEE Int. Pulsed Power Conf. 1993, pp. 835-838.
[14] V.G. Shpak, S.A. Shunailov, M.R. Oulmascoulov, M.I.Yalandin, "Subnanosecond Front, High-Voltage Generator Based on a Combined Pulse Forming Line", Proc. of 11th IEEE Int. Pulsed Power Conference 1997, pp. 1581-1584.
[15] L.H. Bowen, E. G. Farr, J.M. Elizondo, J. Lehr "High-voltage, high rep-rate, low jitter, UWB source with ferroelectric trigger", Proc. 12th IEEE Int. Pulsed Power Conference 1999, pp. 1137-1140.
[16] C.E. Baum, J.J. Sadler, A.P. Stone, "A prolate spheroidal uniform isotropic dielectric lens feeding a circular coax", Electromagnetics, vol. **15** pp. 223-241, 1995.
[17] H. Krompholz, L.L. Hatfield, B. Short, M. Kristiansen, "Sub-nanosecond gas breakdown phenomena in the voltage regime below 15 kV", EUROEM 2000, Edinburgh, UK, June 2000, Ultra-wideband, short pulse electromagnetics 5, P.D. Smith, S.R. Cloude eds., Kluwer Academic/Plenum Publishers, New York 2002, pp.437-444

[18] H. Krompholz, L.L. Hatfield, B. Short, D. Hemmert, M. Kristiansen, J. Mankowski, M. Brown, L. Altgilbers, "Gas Breakdown in the sub-nanosecond regime with voltages below 15 kV", IEEE Transactions on Plasma Science, **30** (2002) 1916]
[19] "Nanosecond pulsed breakdown for point-plane geometries at moderate voltage", H. Krompholz, L. Hatfield, M. Haustein, J. Spears, M. Kristiansen, AMEREM 2002, Annapolis, Md, June 2002, Ultra-wideband, short pulse electromagnetics 6, Eric L Mokole, Mark Kragalott, Karl R Gerlach eds., Springer, New York 2003, pp.409-414
[20] "Sub-nanosecond point-plane gas breakdown in conical shaped spark gap", J. Spears, H. Krompholz, L.L. Hatfield, 29th IEEE International Pulsed Power Conference, Dallas, TX, June 2003]
[21] "Fast Volume Breakdown in Argon and Air at Low Pressures", H. Krompholz, E. Crull, L. Hatfield, A. Neuber, EUROEM 2004, Magdeburg, Germany, July 12-16, 2004, to be published in Ultra-Wideband, Short-Pulse Electromagnetics 7 (UWB SP 7)].
[22] H. Krompholz, L.L. Hatfield, A. Neuber, D. Hemmert, K. Kohl, J. Chaparro, "Sub-nanosecond breakdown in argon at high overvoltages", 15th IEEE International Pulsed Power Conference, Monterey, CA, June 14-17, 2005]
[23] H. Krompholz, L. Hatfield, A. Neuber, K. Kohl, J. Chaparro, " Phenomenology of Subnanosecond Gas Discharges at Pressures below One Atmosphere", IEEE Trans. Plasma Science, **34** (2006), 927-936
[24] H. Krompholz, L. Hatfield, A. Neuber, J. Chaparro, H.-Y. Ryu, "Ultrafast gas breakdown at pressures below one atmosphere", submitted to CEIDP, Kansa City, MO., Oct. 2006
[25] G. Mesyats, "On the similarity law in picosecond gas discharges", JETP Lett. **83**, pp. 19-21, 2006
[26] same as [11], pp. 233-238

6. Appendix

Personnel

PI's/CoPi's:	H. Krompholz
	L. Hatfield
	A. Neuber
Post-Doc:	D. Hemmert
MSEE-students:	E. Crull
	K. Kohl
	J. Chaparro
	W. Justis

Publications

H. Krompholz, L. Hatfield, A. Neuber, K. Kohl, J. Chaparro, " Phenomenology of Subnanosecond Gas Discharges at Pressures below One Atmosphere", IEEE Trans. Plasma Science, **34** (2006), 927-936

"Fast Volume Breakdown in Argon and Air at Low Pressures", H. Krompholz, E. Crull, L. Hatfield, A. Neuber, EUROEM 2004, Magdeburg, Germany, July 12-16, 2004, to be published in Ultra-Wideband, Short-Pulse Electromagnetics 7 (UWB SP 7), F. Sabath ed., Springer 2007 (ISBN 0-387-37728-X).

H. Krompholz, L.L. Hatfield, A. Neuber, D. Hemmert, K. Kohl, J. Chaparro, "Subnanosecond breakdown in argon at high overvoltages", 15th IEEE International Pulsed Power Conference, Monterey, CA, June 14-17, 2005

H. Krompholz, L. Hatfield, A. Neuber, J. Chaparro, H.-Y. Ryu, "Ultrafast gas breakdown at pressures below one atmosphere", CEIDP (Conf. on Electrical Insulation and Dielectric Phenomena), Kansa City, MO., Oct. 2006

Theses

Eric Crull, Masters Thesis, Texas Tech University, Dec. 2004
"Sub-nanosecond Breakdown in Argon and Air at Low Pressure"

Kevin Kohl, Masters Thesis, Texas Tech University, Dec. 2005
"Electrical, optical and x-ray diagnostics of subnanosecond breakdown in gases"
http://etd.lib.ttu.edu/theses/available/etd-11222005-133441/

Jordan Chaparro, Masters Thesis, Texas Tech University, Aug.. 2006
"Ultrafast breakdown at pressures below one atmosphere"
http://etd.lib.**ttu**.edu/theses/available/etd-07252006-124922/unrestricted/**Chaparro**_Jordan_**Thesis**.pdf